5G New Radio for Non-Terrestrial Networks: Analysis and Comparison of HARQ and RLC ARQ Performance Over Satellite Links

IEEE Access
Multidisciplinary | Rapid Review | Open Access Journal

Received 11 March 2025, accepted 2 April 2025, date of publication 24 April 2025, date of current version 5 May 2025.

Digital Object Identifier 10.1109/ACCESS.2025.3563983

RESEARCH ARTICLE

5G New Radio for Non-Terrestrial Networks: Analysis and Comparison of HARQ and RLC ARQ Performance Over Satellite Links

RICCARDO TUNINATO[1,2], (Graduate Student Member, IEEE), GABRIEL MAIOLINI CAPEZ[1], (Graduate Student Member, IEEE), NICOLÒ MAZZALI[2], (Member, IEEE), AND ROBERTO GARELLO[1], (Senior Member, IEEE)

[1]Department of Electronics and Telecommunications, Politecnico di Torino, 10129 Turin, Italy
[2]European Space Research and Technology Centre, European Space Agency, 2201 Noordwijk, The Netherlands

Corresponding author: Roberto Garello (roberto.garello@polito.it)

This work was supported in part by European Space Agency through the Physical Layer Simulator for 5G New Radio and OTFS under Contract 4000141791/23/NL/KK/nh; and in part by European Union—Next Generation EU under Italian National Recovery and Resilience Plan (NRRP), Mission 4, Component 2, Investment 1.3, CUP E13C22001870001, Partnership on "Telecommunications of the Future" (Program "RESTART") under Grant PE00000001.

ABSTRACT In this paper, we study the extension of 5G New Radio (NR) to Non-Terrestrial Networks (NTN). For terrestrial ones, Hybrid Automatic Repeat reQuest (HARQ) is the main retransmission solution used by 5G NR at the physical and MAC layers, enhancing decoding performance through diversity and coding gain. However, for NTN, its implementation faces challenges due to the significant delays caused by the long distances of satellites. In the first part, we begin by investigating the minimum number of HARQ processes required for various LEO scenarios, as well as the relationship between the number of processes and the coherence time of the satellite link. Next, while the performance of 5G retransmission schemes over AWGN and terrestrial channels is well explored, this is not the case for realistic satellite channel models. To address this, we have developed an open-source simulator that accurately implements all the blocks of the data channel transmission and reception chain, including the retransmission schemes and the Land Mobile Satellite (LMS) channel. We consider the 5G NR Physical Downlink Shared Channel (PDSCH) and we present and discuss a number of results over the LMS channel, which are important to understand the HARQ performance for the NTN satellite scenario. In the second part, we consider the 5G NR alternative retransmission solution, RLC ARQ, which is available at the Radio Link Control (RLC) layer. This method might be interesting for satellite links, because it adds minimal complexity to the receiver side, but it provides less enhancement to signal reception capabilities and more latency. We first present an analytic model to compute its performance over the LMS channel, then we analyze its behavior. Finally, we provide a detailed comparison and discussion of HARQ and RLC ARQ performance in terms of block error rate, spectral efficiency, and latency. This extensive analysis provides valuable insights for researchers and space agencies interested in applying 5G NR to satellite-based Non-Terrestrial Networks.

INDEX TERMS Satellite communications, 5G New Radio, Non-Terrestrial Networks, HARQ, ARQ.

I. INTRODUCTION

Traditionally, terrestrial infrastructure forms the backbone of mobile communication networks. However, the growing relevance of Low Earth Orbit (LEO) satellite constellations is leading to their integration into the latest 5G specifications [1]. This convergence offers an effective solution for bridging the digital divide, enabling internet access in remote zones previously underserved by traditional Terrestrial Networks. In addition to closing the digital gap, satellites are

The associate editor coordinating the review of this manuscript and approving it for publication was Tarcisio Ferreira Maciel.

TABLE 1. List of most frequently occurring acronyms.

Application	Maximum latency
ACM	Adaptive Coding and Modulation
BLER	Block Error Rate
HARQ	Hybrid Automatic Repeat reQuest
LEO	Low Earth Orbit
LMS	Land Mobile Satellite
MCS	Modulation Coding Scheme
MEO	Medium Earth Orbit
NR	New Radio
NTN	Non Terrestrial Networks
PDSCH	Physical Downlink Shared Channel
RLC	Radio Link Control
RTT	Round-Trip Time
SCS	Subcarrier Spacing
SE	Spectral Efficiency

also crucial for densely populated areas, bringing additional internet access to big cities, providing a secondary link in case some disruptions affect the terrestrial ones, and for passengers of vessels and aircraft.

In Release 17, the Third Generation Partnership Project (3GPP) introduced Non-Terrestrial Networks (NTNs) in the 5G standard [2], [3]. The main use cases identified for NTN are the following:

- Enhanced Mobile Broadband (eMBB) - backhauling support for underserved areas with limited user throughput, users in isolated villages, passengers on board vessels or aircraft, critical network links as primary or secondary connections, live broadcast and ad-hoc broadcast/multicast streams.
- Massive Machine-Type Communications (mMTC) - enhanced wide area or local area Internet-of-Things services to collect and report local information.

The satellite access network can then be used to serve both fixed and mobile satellite services, and can also be supported by a terrestrial access network (Fig. 1).

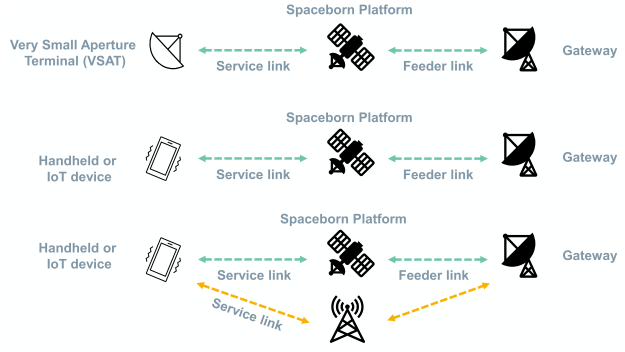

FIGURE 1. Possible satellite access network architectures.

To enable the adoption of 5G for NTN, it is essential to thoroughly examine its performance over satellite links, anticipate its expected behavior, identify potential critical issues, and determine if adaptations are necessary. The new solutions for NTN shall consider the different challenges posed by the user-satellite link, such as high path losses and large delays due to the satellite distances, and the high Doppler shifts due to the satellite speed [4], [5].

In this context, retransmission techniques play a fundamental role in guaranteeing the success of the data exchange. Hybrid Automatic Repeat reQuest (HARQ) is the primary retransmission solution implemented by 5G NR at the physical layer [6] and handled by the Medium Access Control (MAC) layer. It can significantly improve the decoding performance thanks to diversity and coding gains. However, the high delays caused by the satellite distance make its implementation challenging. A different solution is available at the Radio Link Control (RLC) layer, called RLC ARQ [7]. This solution requires negligible additional complexity at the receiver side, but offers also less improvement to the signal reception capabilities. The purpose of this paper is to conduct a thorough analysis and comparison of these two schemes for 5G NTNs.

A. PREVIOUS LITERATURE

For terrestrial networks, HARQ was studied in [8], while in [9] novel protocol architectures were studied to improve HARQ/ARQ latency and reliability. In [10] the HARQ feedback was optimized to enhance the Spectral Efficiency (SE), while in [11] a solution to predict the decoding outcome was designed to anticipate the HARQ feedback transmission and reduce latency for mission-critical communications. A solution to reduce the delay in HARQ was proposed also in [12], namely adaptive HARQ, where the transmitter schedules multiple transmissions together when it experiences a low quality channel, thus decreasing the delay due to retransmissions. Moreover, [13] presents a new solution to decrease the hardware complexity of HARQ at the decoder.

The performance of 5G NTN with LEO satellites was investigated in [14], while four LEO constellations were compared in [15], where authors described their configurations and evaluated their system throughput.

Authors in [16] developed a 5G NTN testbed over Geostationary Orbit (GEO) satellites, and discussed the need of disabling HARQ due to the very large delays. Similarly, [17] shows an experimental study of 5G NTN over GEO satellites, but investigating the performance of retransmissions at RLC level.

For NTNs, latency is a major impairment and is mostly caused by the satellite distance. The 3GPP discussed the enhancements in NTN to solve this criticality of HARQ in [18], considering both the possibility of adapting the number of HARQ processes to cope with the large delays, and the option to disable HARQ, depending on the scenario. Other 3GPP studies focused on the performance of HARQ and its comparison with RLC ARQ, and some results were presented in [19] and further deepened in [20].

These results provide a first baseline for discussing NTN solutions; however, further analysis is needed to comprehensively understand factors such as the number

TABLE 2. Literature comparison.

Reference	Key findings	Gaps
[8], [9], [10], [11], [12]	Analysis of HARQ in 5G and new techniques to improve its performance.	Limited to terrestrial networks.
[13]	Hardware solution to decrease HARQ complexity.	Specific to hardware and no results for NTN scenarios.
[14], [15]	5G NTN performance in LEO.	No impact of retransmission techniques and LMS channel.
[16], [17]	Real world testbed for 5G NTN.	Only satellites in GEO, and HARQ is not considered.
[18], [19], [20]	Study on HARQ and RLC ARQ in NTN.	Different use case (handheld, S-Band, NTN TDL-D channel), and limited number of configurations and results.

of retransmissions, performance, latency, and spectral efficiency.

B. MOTIVATIONS

Retransmission schemes in 5G networks have been thoroughly analyzed for terrestrial networks, but not for satellite ones, characterized by very long distances. Moreover, while the performance of these schemes is well understood in the case of AWGN and terrestrial channels, this is not true for realistic Land Mobile Satellite (LMS) channels.

Given that retransmissions are crucial for extending 5G to non-terrestrial networks, there is a need to evaluate their performance specifically in satellite environments. First of all it is essential to understand the minimum number of HARQ processes required for different LEO scenarios, and the link between the number of processes and the coherence time of the satellite link.

Then it is important to calculate the retransmission performance, and compare HARQ and RLC ARQ schemes over the LMS satellite model to provide quantitative insights into the differences between the two for LEO non-terrestrial networks. Results in terms of block error rate, latency, and spectral efficiency should be made available to researchers and space agencies to fully understand the behavior of the two retransmission schemes in this satellite scenario.

Last but not least, we believe it is important to offer an open-source simulator that models the entire 5G transmission and reception chain for satellite links, including retransmission schemes and LMS model so that researchers can further analyze their performance and explore potential improvements.

C. CONTRIBUTIONS

The scope of this paper is to evaluate and compare the performance of the two 5G NR retransmission protocols, HARQ and RLC-ARQ, over NTN links, considering the specific challenges related to satellite distance and channel modeling. In particular:

- We calculate the minimum number of HARQ processes required for different LEO scenarios and analyze the relationship between the number of processes and the coherence time of the satellite link.
- We have developed and made available an open-source simulator, which includes all the constituent blocks of the PDSCH transmission and reception scheme, both retransmission protocols, and the satellite LMS model.
- We present an extensive set of results on HARQ performance over the LMS channel, clarifying its behavior in NTN scenarios.
- We derive an analytical model to evaluate RLC ARQ over the LMS channel, validate it through simulations, and compute the performance of ARQ over the LMS channel.
- We compare HARQ and RLC ARQ over the LMS channel, offering quantitative insights into their differences for LEO non-terrestrial networks in terms of block error rate, latency, and spectral efficiency.

A thorough analysis of this kind for satellite scenarios is, to our knowledge, entirely novel. We believe these results will be valuable for researchers and space agencies in fully understanding the behavior of the two retransmission schemes in realistic satellite environments, offering useful insights for the extension of 5G to non-terrestrial networks.

D. ORGANIZATION

The paper is organized as follows. Section II presents the scenario adopted for this study and the NTN channel model. Section III introduces the different functional blocks of the PDSCH and the two retransmission techniques, HARQ and RLC ARQ. In Section IV we present the problem setting. In Section V we consider HARQ, we highlight its main issues for NTN, and we present an extensive set of performance results. In Section VI we present an analytic formulation and numerical results for RLC ARQ over the LMS channel. The comparison between the two schemes is further discussed in Section VII. Finally, in Section VIII the conclusions are drawn.

II. SCENARIO AND CHANNEL MODEL

The NTN scenario we are considering in this paper is described in Tab. 3.

The eMBB use case is of particular interest for the satellite industry because of the growing demand for broadband services and the need for global high-speed connectivity. A typical User Equipment (UE) for broadband communications in the Ka-band, which falls within the 3GPP Frequency Range 2 (FR2), requires a directive antenna and an environment with a clear Line-of-Sight (LOS) to the satellite. Such UE is typically denoted as Very Small Aperture

TABLE 3. Considered NTN scenario.

Parameter	Value
NTN service	Enhanced Mobile Broadband (eMBB)
NTN Configuration	Direct access
UE device type	VSAT (20 cm Ka-band)
UE condition	Outdoor, Line-of-Sight (LOS)
UE Antenna Pointing	Satellite-tracking (50 m accuracy)
Payload	Regenerative[1]
Synchronisation	Perfectly synchronized (GNSS-assisted)

[1] Satellite with onboard gNB

Terminal (VSAT), and in the following we will assume for simplicity a perfect satellite-tracking capability and perfect GNSS-assisted synchronization. Although not yet supported by the 3GPP Release 18, regenerative payloads will be included in Release 19 and are considered in this paper to simplify the system architecture under study.

The choice of this scenario guides the selection of the channel model. For 5G NTN, the 3GPP introduced a new channel model in Section VI of TR 38.811 [2]. The characteristics of this channel are:

- Support of the frequency range from 0.5 GHz up to 100 GHz. Two frequency ranges are targeted in particular: FR1 below 6 GHz, and FR2 corresponding to the Ka-band. For the Ka-band, the uplink (UL) frequency is around 30 GHz while the downlink (DL) frequency is around 20 GHz.
- UE mobility. Speeds up to 1000 km/h are supported, implying that aircraft can be served by the satellite.

The channel fading model is influenced by the propagation environment and the user terminal, resulting in either a flat or a frequency-selective fading channel.

As shown in Tab. 3, in this paper we are considering a VSAT terminal as UE with a 20 cm Ka-band antenna. When directive antennas are used, the antenna radiation pattern spatially filters out the multipath generated by the signal reflections coming from non-LOS directions, which typically have higher delays and cause the frequency selectivity of the channel [21]. This assumption is also clearly stated by the 3GPP when considering a VSAT-type UE antenna pattern (Section 6.4.2 of [2]).

As a consequence, we focus on the flat fading model. The description is provided by the 3GPP in [2], Section 6.7, and it is essentially coincident with the LMS ITU channel model [22].

The LMS channel serves as a reliable reference for satellite link simulations, as it is based on extensive real-world measurements across various environments, frequency bands, and satellite elevations. It is based on the concept of two-state fading, where the channel can be in a good or a bad state, depending on the shadowing affecting the direct signal, usually referred to as the LOS component. For our VSAT scenario, we focus on users seeing the channel in the good state and without shadowing. The signal is then characterized by the contribution of a strong LOS component and the multipath, generated by the nearby scatterers, as in the Rice model [23]. The complex multipath component is the fast-varying component of the channel and is characterized by the Doppler spread resulting from the user terminal speed s. The Rician fading can be described by the K-factor, defined as the ratio between the power of the LOS component and the power of the multipath.

In this paper we will focus on:

- K-factor values equal to 15 and 20 dB;
- Terminal speed values equal to 0, 50, 150, 900 km/h;
- LEO satellite altitude equal to 600 km.

III. 5G NTN PDSCH AND RETRANSMISSION TECHNIQUES

In 5G NR, the PDSCH is the physical channel delivering user data [24]. Fig. 2 represents the transmission diagram of the PDSCH physical layer, from data generation to its recovery. In PDSCH the data bits are encoded by Low-Density Parity Check (LDPC) coding, and then modulated as QPSK or QAM symbols depending on the selected Modulation and Coding Scheme (MCS). Finally, they are mapped onto the resource grid together with pilot symbols for channel estimation, called Demodulation Reference Signals (DMRS). More details on PDSCH can be found in [24], [25], and [26].

All the blocks of the transmitter and the receiver were implemented in a Matlab link-level simulator.[1]

A. HARQ

The HARQ protocol is the primary way of handling retransmissions in NR. If the receiver detects errors in the received codeword and/or the transmitter does not receive an acknowledgement (ACK) message, a retransmission can be scheduled. When the receiver is not able to correctly decode the codeword, the received codeword still contains useful information that would be lost if the codeword were discarded. This shortcoming is addressed by HARQ with soft combining: the received codewords are stored in a memory buffer and later combined with the retransmitted versions to obtain a single, combined codeword that is more reliable than its constituents [28]. The LDPC decoder operates then on the combined codeword. Although the protocol itself is primarily handled by the MAC layer [29], soft combining is a physical layer functionality.

For the DL, a maximum of 16 HARQ processes per cell are supported by the UE. Each HARQ process handles up to 3 retransmissions of a codeword, for a total of 4 transmissions. In 5G NR, each transmission corresponds to a different Redundancy Version (RV), in the order {0 2 3 1}. For each redundancy version, the set of bits to be transmitted is different, and this is why HARQ has a coding gain. A circular buffer, represented in Fig. 3, is used to store and select the bits to be transmitted for each RV.

[1] The Matlab code of the 5G NTN PDSCH HARQ/ARQ simulator used to obtain the paper's results is available at [27].

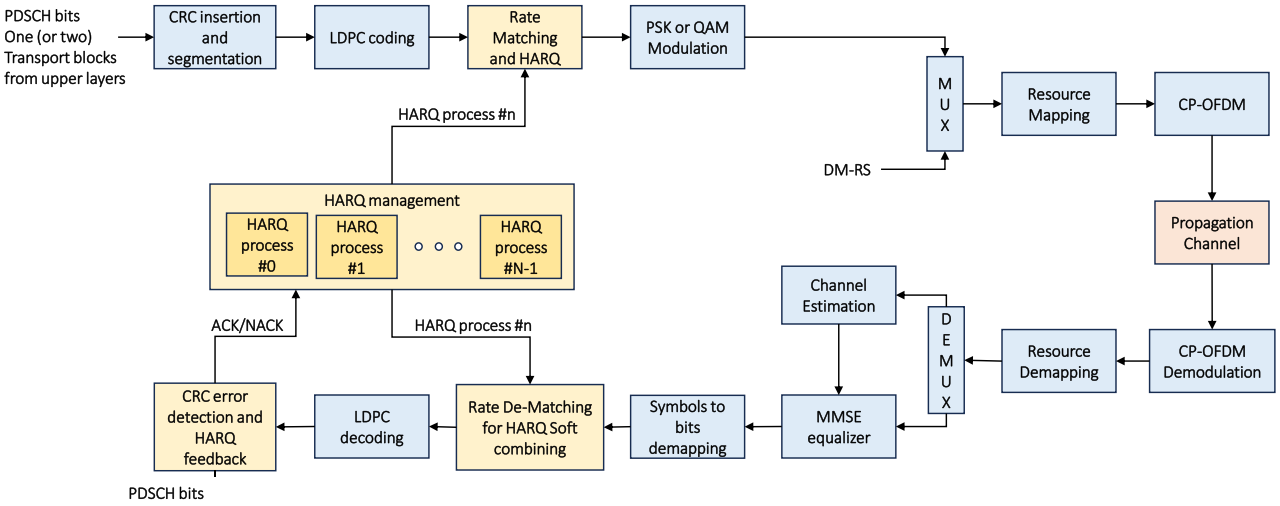

FIGURE 2. PDSCH block scheme.

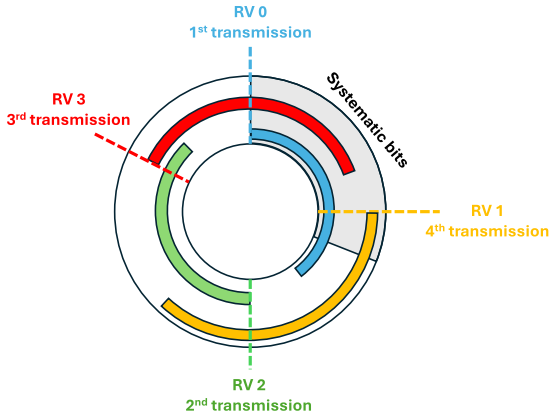

FIGURE 3. Circular buffer and redundancy versions for HARQ transmissions.

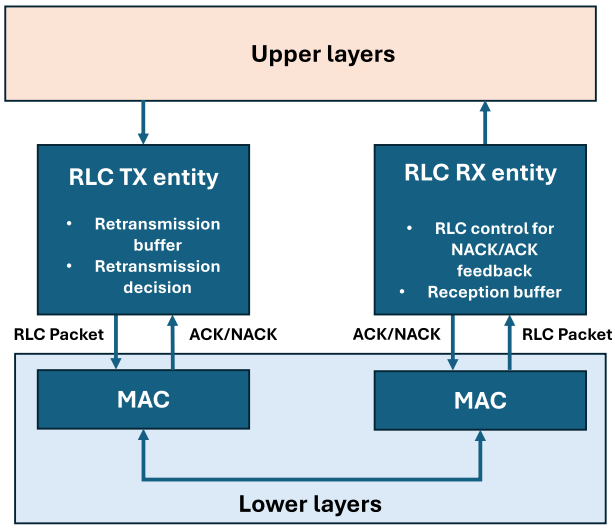

FIGURE 4. RLC transmitting (TX) and receiving (RX) entities.

B. RLC ARQ

RLC ARQ is a retransmission protocol at the RLC layer of the 5G stack, above the MAC layer. Differently from HARQ, this protocol does not exploit previous transmissions to improve the decoding, i.e., it is memoryless. This means that no coding or diversity gain can be obtained. However, it does not need to store all the data at the receiver side, providing a much lower complexity than HARQ. For RLC ARQ, up to 32 transmissions of the same codeword are possible. Details on RLC and the ARQ retransmission mechanism are reported in [7]. Fig. 4 shows a simplified representation of the ARQ mechanism at the RLC layer. Two RLC entities, one at the transmitter side and one at the receiver side, manage the packet buffer, the ACK/NACK feedback, and the retransmission decision.

IV. PROBLEM SETTING

Tab. 4 reports the main transmit, channel, and receive parameters used in this paper to evaluate the performance of the HARQ and RLC ARQ protocols on the PDSCH. It also contains the main parameters for the configuration of the DMRS. Please note that for the following results, the channel estimation is considered perfect, i.e., genie-aided, and not based on the DMRS.

The metrics we are using to evaluate the performance of 5G NTN are the following.

- **Block Error Rate (BLER)**: It is defined as the ratio of the number of correctly decoded TBs $N_{\text{TB,CD}}$ over the total number of transmitted TBs $N_{\text{TB,TX}}$:

$$\text{BLER} = N_{\text{TB,CD}}/N_{\text{TB,TX}}.$$

- **Spectral Efficiency (SE)**: In general, the nominal SE can be defined as:

$$\text{SE} = \frac{k}{n}\log_2(M) \quad \left[\frac{bit}{s \cdot Hz}\right] \tag{1}$$

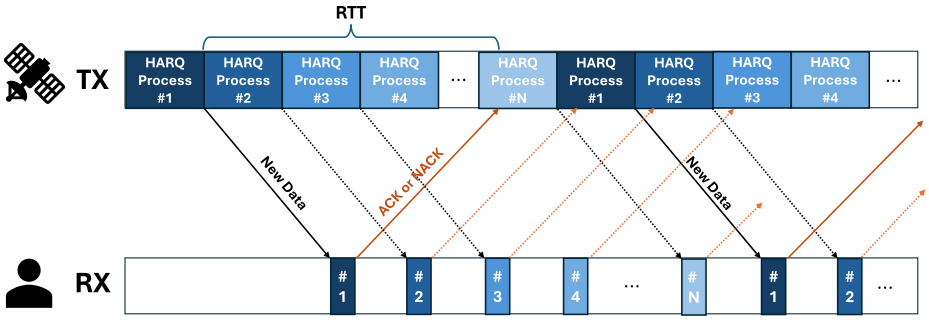

(a) N is equal to the number of HARQ processes required to cover the entire RTT.

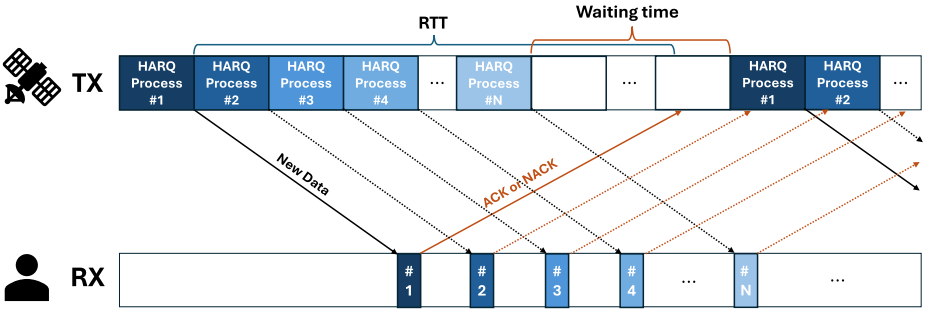

(b) N is less than the number of HARQ processes required to cover the entire RTT. This results in a waiting time.

FIGURE 5. Latency with N HARQ processes and different Round Trip Times.

where k is the number of information bits, n is the number of coded bits, and M is the modulation order. This expression does not take into account the impact of errors on the actual rate achievable by the system. We then define an SE based on the concept of goodput, i.e., we consider the number of correctly received information bits over the total transmission time:

$$\mathrm{SE}_{GP} = \frac{N_{\mathrm{TB,CD}} N_{b/\mathrm{TB}}}{BT} \quad \left[\frac{bit}{s \cdot Hz}\right] \tag{2}$$

where $N_{b/\mathrm{TB}}$ is the number of information bits per TB, B is the signal bandwidth, and T is the time interval considered for the computation of the SE. T can be computed as $T = T_{\mathrm{OFDM\ sym}} \cdot N_{\mathrm{OFDM\ sym}} = T_{slot} \cdot N_{slots}$, where $T_{\mathrm{OFDM\ sym}}$ is the duration of an OFDM symbol (in seconds), $N_{\mathrm{OFDM\ sym}}$ is the number of OFDM symbols that fit in T, T_{slot} is the slot duration (in seconds), and N_{slots} is the number of slots that fit in T. All the results in this paper refer to this definition of SE.

- **Latency**: A representation of the modelled delay can be seen in Fig. 5. In order to estimate the latency caused by the user-satellite distance as a function of the number of retransmissions N_{ReTx}, we adopt the following formula:

$$\begin{aligned} L(N_{ReTx}) &= (N_{ReTx}+1)T_{slot} + T_{slot} \cdot \lceil T_p/T_{slot} \rceil \\ &\quad + T_{slot} \cdot \lceil T_p/T_{slot} \rceil \cdot 2N_{ReTx} \\ &= (N_{ReTx}+1)T_{slot} \\ &\quad + T_{slot} \cdot \lceil T_p/T_{slot} \rceil \cdot (2N_{ReTx}+1) \end{aligned} \tag{3}$$

where T_p is the propagation delay due to the satellite distance d, computed as $T_p = d/c$ where c is the speed of light, and the ceiling operation $\lceil x \rceil$ returns the first integer equal or greater than x. In the right-hand side of Eq. (3), the first term takes into account the time required for the slot to be transmitted, while the other terms correspond to the propagation time of the first transmission, plus the propagation time of the NACK and the successive retransmissions. The ceiling operator guarantees that the actual time consumed by the propagation must be a multiple of the slot time, since the system considers slot-based transmissions.[2] Note that this latency is measured at the receiver side, neglecting the additional delay caused by an ACK transmission (i.e., after successful decoding) or the last ACK/NACK transmission. We overlook the extra delay caused by UE or gNB processing. Therefore, the latency obtained with Eq. (3) is a lower bound for the actual system latency.

V. RESULTS FOR HARQ

The HARQ designed for NR presents some critical issues when adopted for NTN, due to the larger delays caused by the satellite distance. In our study, we focus on regenerative payloads and account for only the propagation delay in the user-satellite link as the Round-Trip Time (RTT), excluding

[2]Both gNB and UE must wait for the fraction of the slot currently processed before transmitting the new one.

TABLE 4. PDSCH and receiver configuration.

Parameter	Value
Frequency band	Ka-band
Carrier frequency DL	20 GHz
Carrier frequency UL	30 GHz
Symbol allocation	14 per slot
Numerology μ	3
Transmission Time Interval (TTI) T_{slot}	0.125 ms
Subcarrier Spacing Δf	120 kHz
NPRB	140
Bandwidth	201.6 MHz
HARQ	Enabled
HARQ max processes	Adapted to RTT
Satellite orbit	LEO 600 km
Channel model	LMS
K-factor	{15, 20} dB
Terminal speed s	{0, 50, 150, 900} km/h
CP duration	0.59 μs
Mapping Type	A
Number of Layers	1
Number of TX antennas	1
Number of RX antennas	1
Number of codewords per TB	1
Maximum LDPC iteration count	25
LDPC algorithm	Layered Belief Propagation
RX Equalizer	MMSE
PTRS	Disabled
Channel estimation	Perfect
VRB To PRB Interleaving	Disabled
HARQ redundancy version	[0 2 3 1]
DMRS Type A Position	2
DMRS Length	1
DMRS Additional Position	0
DMRS Configuration Type	1
Number of CDM Groups w/o Data	1

delays associated with the ground station feeder link. While the RTT in terrestrial networks is of the order of a few milliseconds, the propagation delays in NTN are much longer, ranging from several to hundreds of milliseconds depending on the satellite orbit. Due to these larger delays resulting from the user-satellite distance, HARQ may cause an under-utilization of the available resources. Indeed, if the transmitter reaches the maximum number of HARQ processes, it has to wait until the first ACK is received before restarting to transmit. This kind of approach is called stop-and-wait, and the waiting time may result in a significant throughput drop. A simplified representation of the HARQ mechanism and the use of different N HARQ processes can be seen in Fig. 5.

This problem was pointed out during 3GPP meetings and at this time an agreed solution is not available yet. However, two potential solutions were studied [18], [30]. The first is to allow the disabling of HARQ. The second is to optimize HARQ for NTN, avoiding the reduction in peak data rates, by following one of these approaches:

- Increase the number of HARQ processes to match the longer satellite RTT and avoid the stop-and-wait in HARQ. A proposed increased number of supported HARQ processes is 32 [20], but it may be insufficient for many NTN deployments (see analysis in the next section).
- Disable the UL HARQ feedback (ACK/NACK) to avoid the stop-and-wait and rely instead on RLC ARQ.

In the following, we analyze the number of HARQ processes and how that relates to the channel coherence time.

A. ANALYSIS OF THE NUMBER OF HARQ PROCESSES FOR NTN

In this section, we compute and discuss the number of HARQ processes required to fill the RTT. The minimum number of HARQ processes N_{min} required to avoid waiting times, and thus resource wasting, is

$$N_{min} = \lceil 2T_p/T_{slot} \rceil + 1.$$

Examples of N_{min} values for different satellite altitudes, elevation angles θ, and Sub-Carrier Spacings (SCS) are reported in Tab. 5. The cases exceeding the maximum number of 32 HARQ processes, leading to stop-and-wait, are in bold.

From these results we can state that HARQ can be still a solution for LEO, but for lower SCS, corresponding to Frequency Range (FR) 1 of 5G: a maximum of 60 kHz at 600 km altitude and a maximum of 30 kHz at 1200 km altitude. Thus, there are deployments which can still use HARQ without wasting resources. An example are the deployments for handheld devices, operating at lower frequency bands, as L-band and S-band. Instead, HARQ should not be used for Medium Earth Orbit (MEO) satellites. The number of HARQ processes in different NTN use cases are also discussed in [20] and [31].

TABLE 5. Minimum number of HARQ processes required for different scenarios (regenerative payloads).

		LEO 1 θ		LEO 2 θ		MEO θ	
SCS [kHz]	T_{slot} [ms]	90°	30°	90°	30°	90°	30°
15	1	5	9	9	15	**55**	**69**
30	0.5	9	16	17	28	**108**	**136**
60	0.25	17	30	**33**	**55**	**215**	**270**
120	0.125	**33**	**59**	**65**	**108**	**428**	**539**
240	0.0625	**65**	**116**	**129**	**215**	**855**	**1077**

LEO 1: 600 km altitude
LEO 2: 1200 km altitude
MEO: 8000 km altitude

B. ANALYSIS OF CHANNEL COHERENCE TIME

Another aspect that is important to investigate is the temporal coherence of the satellite link between different retransmissions. An upper bound of the coherence time is $1/f_m$, where f_m is the maximum Doppler shift, defined as $f_m = vf_c/c$, where f_c is the carrier frequency. A more practical definition of the coherence time is usually much shorter, as for Clarke's model [32], where $T_c = \sqrt{9/(16\pi f_m^2)} \approx 0.423/f_m$. In Tab. 6 we report the channel coherence time for different terminal speeds s (Ka-band), while Tab. 7 contains the number of HARQ processes that can be considered experiencing a correlated channel (computed as T_c/T_{slot}), depending on the numerology μ. Since a HARQ process

utilizing all the retransmissions requires at least three RTTs, there are no cases where all the HARQ transmissions experience correlated channel realizations.

TABLE 6. Time coherence for different terminal speeds.

Terminal speed s [km/h]	Doppler shift f_m [Hz]	Coherence Time T_c [ms]
5	92.6	11
50	926	1.1
150	2780	0.36
900	16680	0.06

TABLE 7. Number of HARQ processes within one coherence time for different SCSs and speeds.

SCS [kHz]	T_{slot} [ms]	5 km/h	50 km/h	150 km/h	900 km/h
15	1	11	1.1	0.36	0.06
30	0.5	22	2.2	0.72	0.12
60	0.25	44	4.4	1.44	0.24
120	0.125	88	8.8	2.88	0.48
240	0.0625	176	17.6	5.76	0.96

C. HARQ PERFORMANCE VS. NUMBER OF RETRANSMISSIONS

To analyse the performance of the HARQ mechanism we implemented a link-level simulator for the 5G PDSCH described in Section III, based on MATLAB 5G Toolbox [33]. Our first objective is to highlight the benefits of HARQ in terms of BLER and SE, with different numbers of maximum retransmissions N_{ReTx}^{Max}, from 0 to 3. We adopt the LMS channel with $K = 15$ dB and user speed $s = 50$ km/h, for two MCSs from Tab. 8:

- Fig. 6 for MCS A, corresponding to QPSK with code rate 1/2.
- Fig. 7 for MCS B, corresponding to 256QAM with code rate 8/9.

It can be seen in both cases that each retransmission shifts the BLER curve toward lower values of E_s/N_0, at the cost of a lower SE. Moreover, the gain provided by each retransmission is different for the two MCSs, with QPSK showing a total gain of more than 8 dB at BLER $= 10^{-2}$, while for 256QAM the total gain is almost 18 dB.

TABLE 8. The set of MCSs used for the analysis.

MCS index	Modulation	Target code rate	Nominal SE [bit/s/Hz]
A	QPSK	1/2	1.00
B	16QAM	2/3	2.67
C	64QAM	3/4	4.50
D	256QAM	8/9	7.11

The difference in HARQ gains between different MCSs is caused by the different coding gains obtained with the HARQ incremental redundancy, which depends on the nominal code rate. The higher the initial nominal code rate, the higher the coding gain provided by the HARQ incremental redundancy: at each retransmission, more new redundancy bits are added to the codeword at the receiver.

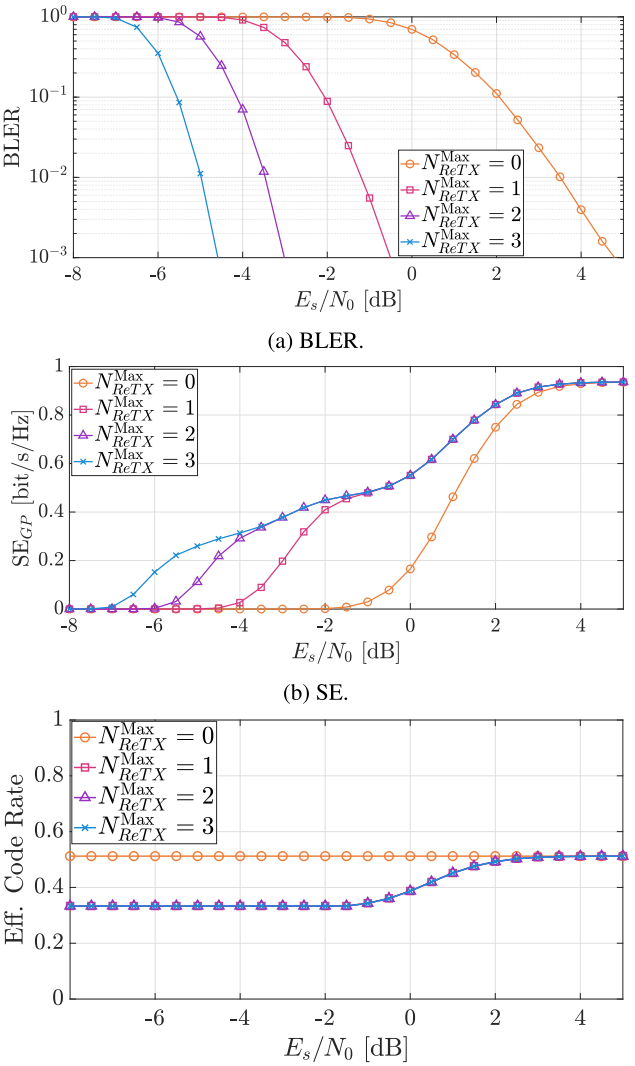

(a) BLER.

(b) SE.

(c) Effective Code Rate.

FIGURE 6. Performance of HARQ for MCS A (QPSK-1/2) and different N_{ReTx}^{Max}. LMS channel with $K = 15$ dBand user speed $s = 50$ km/h.

The variation of code rate at each retransmission can be tracked with a measure that we denote as effective code rate, reported in Fig. 6c and Fig. 7c, for QPSK and 256QAM, respectively. It is defined as the ratio between the amount of unique systematic bits cumulatively transmitted by each RV, and the total amount of unique bits (which include both the systematic bits and the redundancy bits of each RV), counting only once the bits that were transmitted multiple times.

D. HARQ PERFORMANCE VS. DIFFERENT SCENARIOS

Another important aspect that can impact the PDSCH performance is the channel condition, which can vary in different scenarios. Thus, we evaluate the SE performance

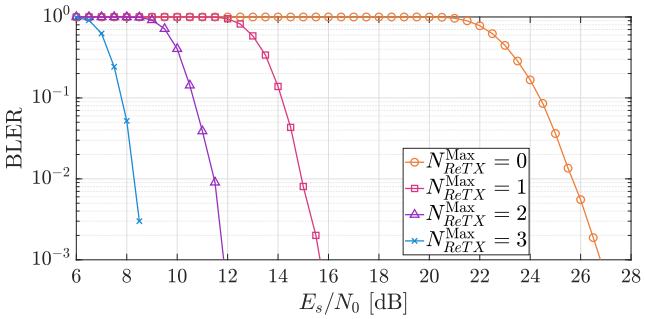

(a) BLER.

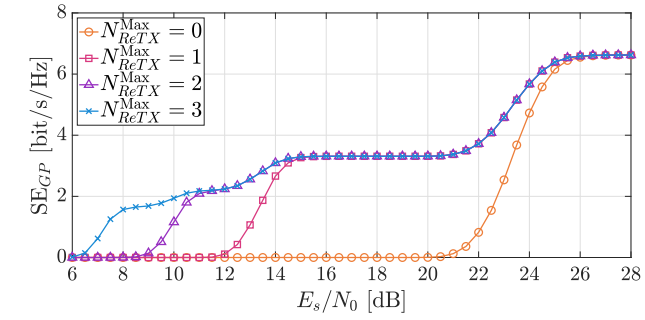

(b) SE.

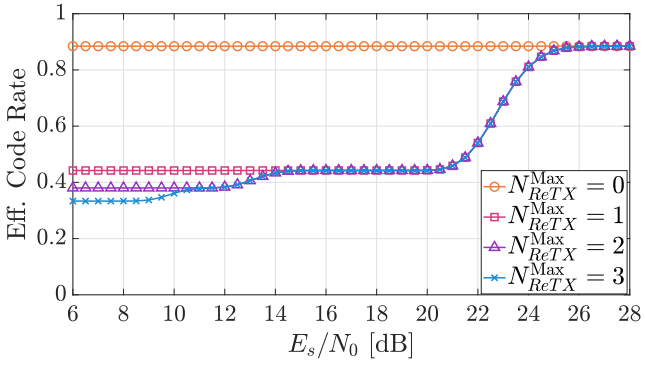

(c) Effective Code Rate.

FIGURE 7. Performance of HARQ for MCS D (256QAM-8/9) and different N_{ReTx}^{Max}. LMS channel with $K = 15$ dBand user speed $s = 50$ km/h.

also with different parameters of the LMS channel, as the Rician K-factor (15 dB and 20 dB) and the user terminal speed s (0, 50, 150 and 900 km/h), for all the four different MCS reported in Tab. 8:

- Fig. 8a for MCS A, corresponding to QPSK with code rate 1/2.
- Fig. 8b for MCS B, corresponding to 16QAM with code rate 2/3.
- Fig. 8c for MCS C, corresponding to 64QAM with code rate 3/4.
- Fig. 8d for MCS D, corresponding to 256QAM with code rate 8/9.

In this case, N_{ReTx}^{Max} is set to 3. With the assumptions in Tab. 4, the UE speed from 0 to 150 km/h influences the performance only marginally. At very high terminal speed (900 km/h) there is a trade-off. High speed typically translates into a larger Doppler spectrum, and thus into higher Intercarrier Interference (ICI) among the subcarriers. On the other hand, having a larger Doppler spectrum means that the channel coherence time is shorter. This may be beneficial since it means that deep fade events are shorter and affect fewer samples. We can observe that for the curves corresponding to the largest user speed (900 km/h), the SE is practically lower for the entire E_s/N_0 interval, but the curve tends to be steeper than the lower speed cases.

E. HARQ PERFORMANCE VS. NUMBER OF HARQ PROCESSES

As reported in Tab. 5, different orbits require different numbers of N HARQ processes. The impact on SE when the maximum number of processes is limited to 32 can be seen in Fig. 9 (for subcarrier spacing 120 kHz and elevation angle 90°). The loss in terms of SE is significant, due to the amount of time resources wasted during stop-and-wait. Given a certain orbit by system design, possible solutions are to increase the number of maximum HARQ processes, to use lower SCS, or to disable HARQ.

VI. RESULTS FOR RLC ARQ

In this section we present the performance of RLC ARQ. First, we derive an analytic model to compute the BLER of RLC ARQ over the LMS channel, starting from the BLER over the Additive White Gaussian Noise (AWGN) channel. Then we present and discuss a set of results. The set of MCSs considered in the following is reported in Tab. 9. It lists the first 17 MCSs defined by 3GPP for PDSCH in [6], which correspond to all the MCSs using QPSK or 16QAM. We select this subset considering the DL link budget provided in Table 6.1.3.3-1 of [30], reporting a carrier-to-noise-ratio of about 8.5 dB with 30° satellite elevation. This link budget does not consider implementation losses, imperfect synchronization, and fading. Thus, despite the use of higher MCSs should not be excluded a priori, it is considered less realistic and therefore not included for this analysis.

A. AN ANALYTICAL MODEL FOR RLC ARQ

Let us assume that the BLER over the AWGN channel is known. For simplicity, we denote γ_{th} the E_s/N_0 value at which the BLER on the PDSCH over the AWGN channel reaches a certain threshold. The LMS channel realization h is Rician-distributed as $h \sim Rice(\nu, \sigma_{\text{MP}})$, with ν the amplitude of the LOS component and σ_{MP}^2 the multipath power (per in-phase/quadrature component). The K-factor of the Rician distribution is defined as $K = \nu^2/2\sigma_{\text{MP}}^2$. Over the LMS channel, the instantaneous received E_s/N_0 can be expressed as

$$\left(\frac{E_s}{N_0}\right)_{RX} = |h|^2\gamma$$

where h is the instantaneous channel gain, and γ is the nominal E_s/N_0 without fading. An approximation of the probability of failed decoding of a codeword can be computed

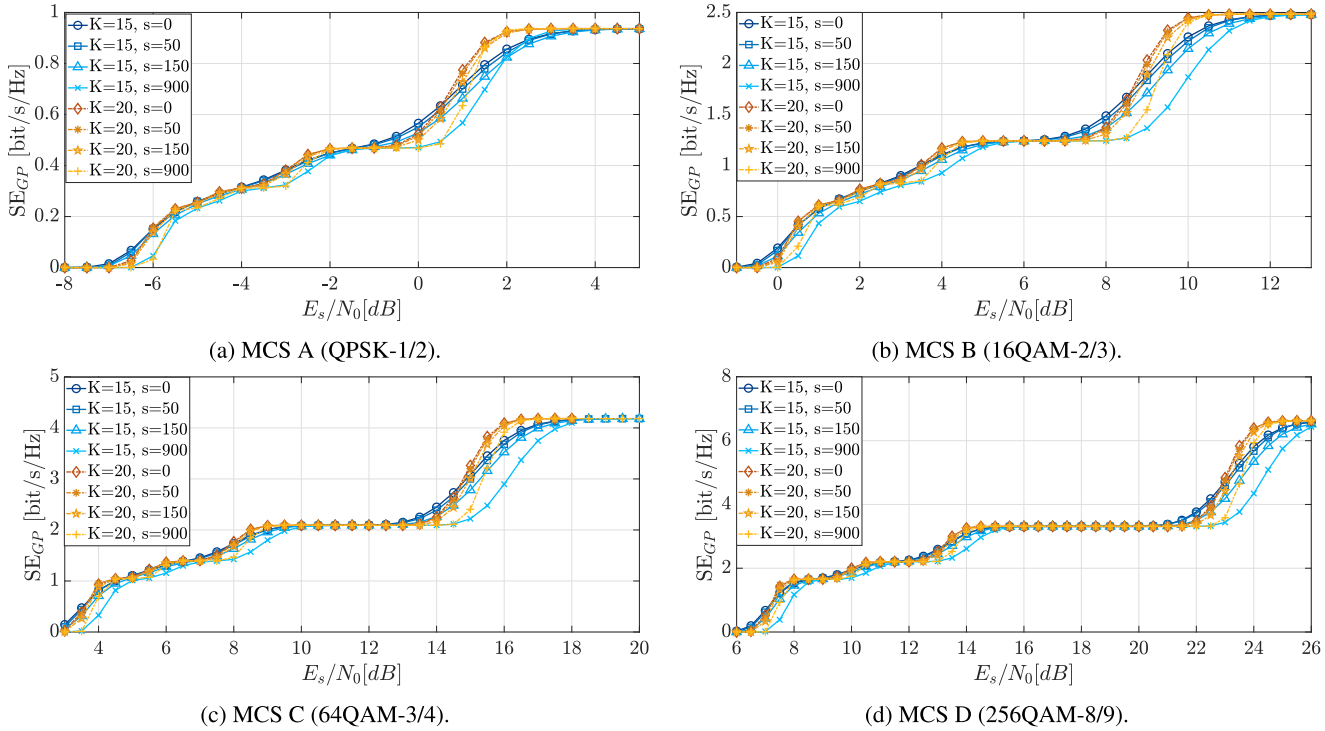

(a) MCS A (QPSK-1/2).

(b) MCS B (16QAM-2/3).

(c) MCS C (64QAM-3/4).

(d) MCS D (256QAM-8/9).

FIGURE 8. HARQ Spectral Efficiency results for different MCS uses cases and different scenarios.

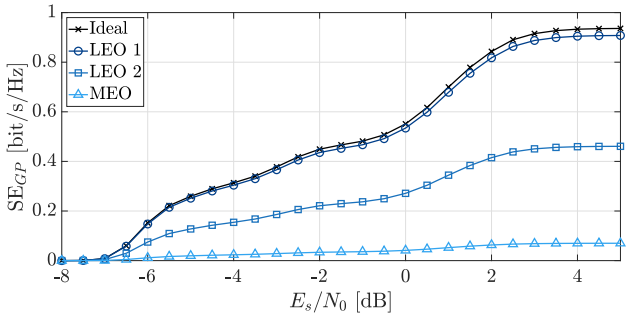

FIGURE 9. HARQ SE for different satellite orbits. MCS A (QPSK-1/2), LMS channel with $K = 15$ dB, $s = 50$ km/h, and $\theta = 90°$.

by assuming a threshold behavior of the decoder: when the instantaneous received E_s/N_0 (assumed constant over a whole codeword) is above the threshold γ_{th}, the decoding is successful; otherwise it is not. We set the threshold so that the corresponding BLER is 10^{-2}: over the AWGN channel, the BLER curve is very steep, so it can be approximated by a step function where the transition from 1 to 0 occurs at γ_{th}. The probability of failed decoding can be reformulated as follows:

$$P\left\{\left(\frac{E_s}{N_0}\right)_{RX} \leq \gamma_{th}\right\} = P\left\{|h|^2 \leq \frac{\gamma_{th}}{\gamma}\right\}. \tag{4}$$

Eq. (4) is the Cumulative Distribution Function (CDF) of $Y = |h|^2$, which is a scaled non-central χ^2-distributed random variable with two degrees of freedom. From [34], this CDF

TABLE 9. PDSCH QPSK MCS from Tab. 5.1.3.1-1 of [6].

MCS index	Modulation	Target code rate $R\times[1024]$	Nominal SE [bit/s/Hz]
0	QPSK	120	0.2344
1	QPSK	157	0.3066
2	QPSK	193	0.3770
3	QPSK	251	0.4902
4	QPSK	308	0.6016
5	QPSK	379	0.7402
6	QPSK	449	0.8770
7	QPSK	526	1.0273
8	QPSK	602	1.1758
9	QPSK	679	1.3262
10	16QAM	340	1.3281
11	16QAM	378	1.4766
12	16QAM	434	1.6953
13	16QAM	490	1.9141
14	16QAM	553	2.1602
15	16QAM	616	2.4063
16	16QAM	658	2.5703

can be expressed as:

$$F_Y(y) = \begin{cases} 1 - Q_1\left(\frac{\nu}{\sigma_{\text{MP}}}, \frac{\sqrt{y}}{\sigma_{\text{MP}}}\right) & \text{if } y > 0 \\ 0 & \text{otherwise} \end{cases}$$

where $Q_1(.)$ denotes the Marcum Q-function. From this CDF, the probability of correct decoding for RLC ARQ with N_T

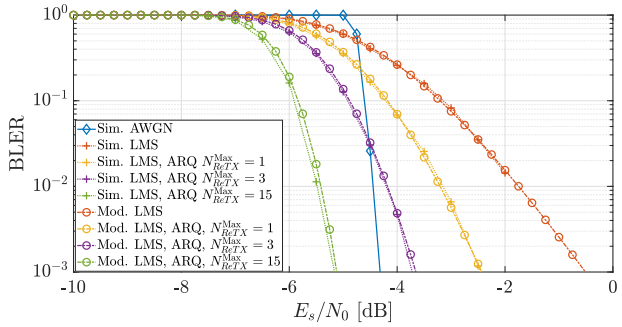

FIGURE 10. Simulated and analytical BLER for MCS 2 (QPSK-193/1024) with RLC ARQ, in AWGN or LMS channel with $K = 15$ dB and $s = 50$ km/h.

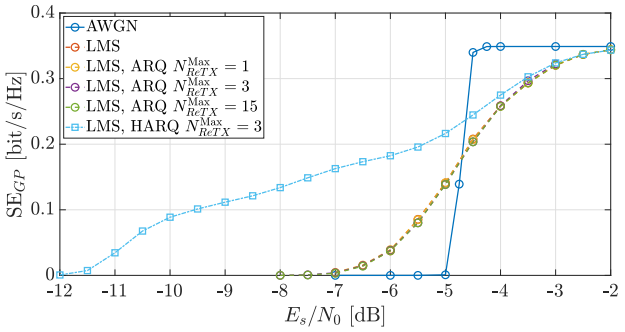

FIGURE 11. SE RLC ARQ and HARQ for MCS 2 (QPSK-193/1024), in AWGN or LMS channel with $K = 15$ dB and $s = 50$ km/h.

transmissions can be computed as:

$$P_c(\gamma, N_T) = \sum_{m=0}^{N_T-1} \left(1 - F_Y\left(\frac{\gamma_{th}}{\gamma}\right)\right) F_Y^m\left(\frac{\gamma_{th}}{\gamma}\right) = 1 - F_Y^{N_T}\left(\frac{\gamma_{th}}{\gamma}\right).$$

Finally, the BLER for a given E_s/N_0 value γ is given by $1 - P_c(\gamma, N_T)$.

B. NUMERICAL RESULTS FOR RLC ARQ

For our tests, as reference, we select MCS 2 of Tab. 9, corresponding to QPSK with rate 193/1024, and we set the LMS channel with K-factor 15 dB and user speed s 50 km/h. This configuration is particularly relevant since it represents a mobile scenario with vehicles at medium-low speed, typical of urban and suburban environments. However, the results can be generalized for any MCS. The performance results obtained with the Matlab PDSCH simulator are then compared with the analytic result derived in the previous section in Fig. 10. The blue curve corresponds to the AWGN performance with a single transmission and it is used to obtain the LMS analytic curves. The BLER curves from the analytical model and the Montecarlo simulations closely overlap. As expected, the probability of correct detection can be increased by increasing the number of retransmissions.

As for the SE, it is depicted in Fig. 11. An important aspect of the RLC ARQ is that the goodput SE, for a certain E_s/N_0 value, is not affected by the number of retransmissions,

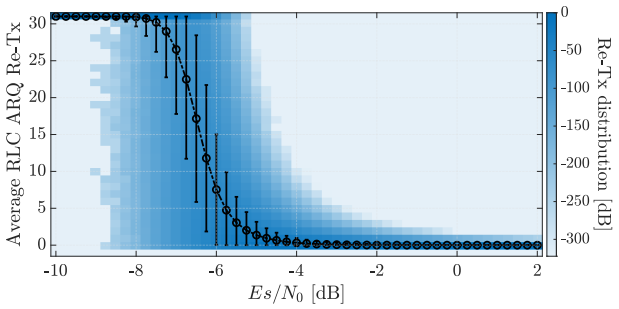

FIGURE 12. RLC ARQ transmission distribution for MCS 2 (QPSK-193/1024), in LMS channel with $K = 15$ dB and speed $s = 50$ km/h.

since the decoding of each TB is independent, even when it is a retransmission. The analytical expression for the goodput SE of RLC ARQ with N^{Max}_{ReTx}, denoted as SE^{ARQ}_{GP}, can be obtained from the definition in Eq. (2) by some considerations and algebraic manipulations, yielding:

$$SE^{ARQ}_{GP}\left(\gamma, N^{Max}_{ReTx}\right) = SE \cdot P_c\left(\gamma, 1\right) \quad \forall N^{Max}_{ReTx}.$$

The independence between retransmissions can also be seen by the probability distribution of the number of retransmissions required at certain E_s/N_0 levels.

This result is reported in Fig. 12, where we set the maximum number of RLC ARQ transmissions to 32. When the E_s/N_0 drops below -4 dB, the number of required transmissions starts spreading almost uniformly from 1 to 32, and then stabilizes at the maximum number when the E_s/N_0 is too low to decode correctly.

VII. COMPARISON BETWEEN HARQ AND RLC ARQ

In this section we compare and discuss the performance of HARQ and RLC ARQ, first for a single MCS and then for a set of MCSs with an Adaptive Coding and Modulation (ACM) mechanism.

A. RESULTS FOR HARQ VS RLC ARQ - SINGLE MCS

We first compare HARQ and RLC ARQ for a single MCS, with the same setting as before (MCS 2 and LMS channel with $K = 15$ dB and user speed $s = 50$ km/h).

The results for the BLER are reported in Fig. 13. From these curves, the advantage of using HARQ instead of RLC ARQ is noticeable. While HARQ shifts the BLER curve by several dBs thanks to the diversity and coding gains, the RLC ARQ is only capable of increasing the steepness of the BLER curve of the single transmission. In the E_s/N_0 range where the BLER for the single transmission is already 1 (Fig. 13, below $E_s/N_0 = -7.5$ dB), RLC ARQ is not able to guarantee a successful decoding.

The comparisons for the SE over the LMS channel, reported in Fig. 11, show that the SE with HARQ is always equal or higher than the one with RLC ARQ. However, the SE gain becomes relevant at low E_s/N_0, where the BLER for a single transmission starts increasing. This means that HARQ extends the operational E_s/N_0 range of any MCS by including

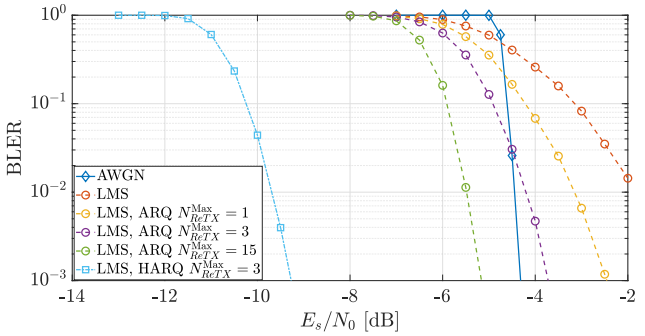

FIGURE 13. BLER of RLC ARQ and HARQ for MCS 2 (QPSK-193/1024), in AWGN or LMS channel with $K = 15$ dB and $s = 50$ km/h.

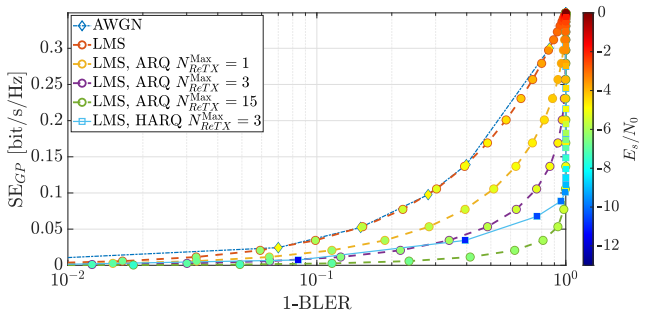

FIGURE 14. SE of RLC ARQ and HARQ for MCS 2 (QPSK-193/1024) over LMS channel with $K = 15$ dB and $s = 50$ km/h.

lower E_s/N_0 values. To better highlight the behavior of the SE with respect to the number of retransmissions, we also plot the SE curves as a function of 1-BLER in Fig. 14. Moreover, we color-coded markers to represent the E_s/N_0 levels in the different SE curves. Different aspects can be observed:

- The two curves without retransmissions (one over AWGN and one over LMS, the blue and the red curve, respectively) have the same behavior since the plotted SE is just the probability of correct decoding multiplied by the nominal SE of the MCS as in Eq. (1). However, the two curves correspond to different E_s/N_0 values, as can be seen by the different colors of the markers (circles for LMS and diamonds for AWGN).
- The SE of RLC ARQ depends on the maximum number of retransmissions. The higher this number, the lower the BLER for a given value of SE (and of E_s/N_0). On the other hand, for a given BLER, the SE can be increased by reducing the maximum number of retransmissions and increasing the E_s/N_0.
- For HARQ, the E_s/N_0 value for a certain BLER is much lower than all the corresponding E_s/N_0 values for RLC ARQ. This can be seen by comparing the colors of the circles (for RLC ARQ) and the squares (for HARQ). Moreover, the HARQ curve approaches the RLC ARQ curve with 4 transmissions (the purple dashed curve) for higher BLER, since also HARQ is using 4 transmissions at those BLER values, resulting in equivalent SE values.

The latency for the same different cases (in terms of mechanism and number of retransmissions) is shown in Fig. 15. The latency with RLC ARQ reaches its maximum in a single transition, over the E_s/N_0 range corresponding to the BLER increase. On the other hand, HARQ results in a multi-step transition, where each step is related to the need for an additional retransmission. This is the same trend shown by the SE in Figs. 6 (b), 7 (b), and 8. Moreover, exploiting very large numbers of maximum retransmissions for RLC ARQ can be very harsh on the latency, and may not be acceptable for many kinds of applications.

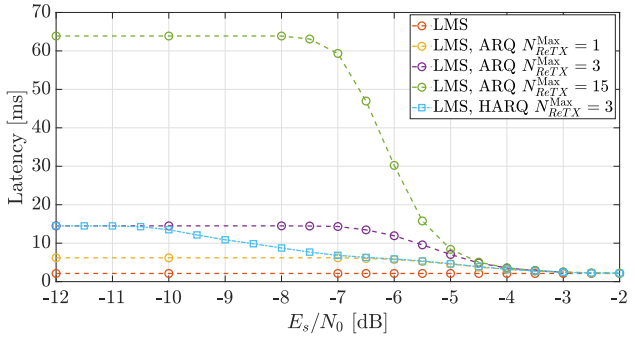

FIGURE 15. Latency comparison of RLC ARQ and HARQ, MCS 2. LMS channel, in LMS channel with $K = 15$ dB and $s = 50$ km/h.

B. RESULTS FOR HARQ VS RLC ARQ - SET OF MCSs

In the following tests, we assume an ACM mechanism is adopted by the system. The ACM selects the appropriate MCS that satisfies a certain BLER threshold and maximize the SE. The selected MCS is kept fixed for all the HARQ retransmissions. This ensures the correct functioning of the HARQ scheme, and it is also reasonable since the state fading duration is typically larger than the time interval required for retransmissions. The average durations of fading states for the LMS channel, from real-world measurements in different environments and computed as in Eq. (17a) of [22], are reported in Tab.10.

TABLE 10. LMS average good state durations at 20 GHz and elevation 30° [22].

Environment	User speed	Average state duration
Train	250 km/h	372 ms
Highway	130 km/h	556 ms
Suburban	70 km/h	1.038 s
Urban	50 km/h	2.652 s

To limit the complexity of the simulations, we consider only MCSs with the same modulation (QPSK) but different code rates, i.e., the entire set of MCSs reported in Tab. 9.

We define the envelope of the SE as the maximum SE among all the MCSs for any E_s/N_0 value, for a target maximum BLER. In our simulations, this target BLER is set to 10^{-3}. The results for the SE envelope are shown in Fig. 16, where HARQ provides a clear SE improvement for very low E_s/N_0 values (i.e., below -7 dB), and it also provides a slight improvement between -7 dB and 1 dB. This small boost can

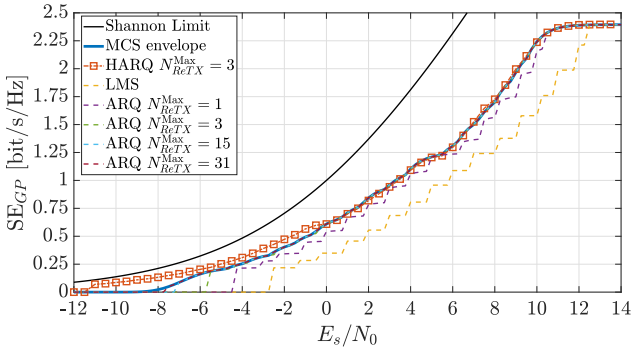

FIGURE 16. SE envelope comparison of RLC ARQ and HARQ, for MCS from 0 to 9, in LMS channel with $K = 15$ dB and $s = 50$ km/h. Target BLER 10^{-3}.

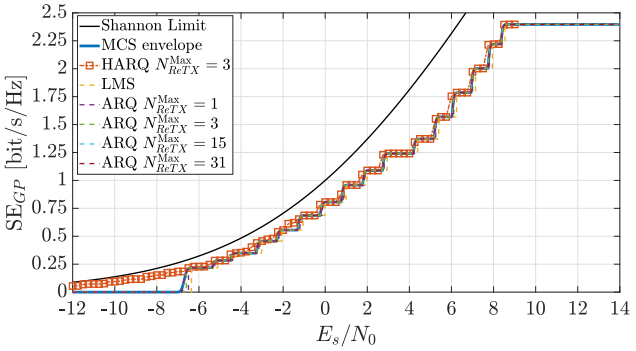

FIGURE 18. SE envelope comparison of RLC ARQ and HARQ, for MCS from 0 to 16, over AWGN channel. Target BLER 10^{-3}.

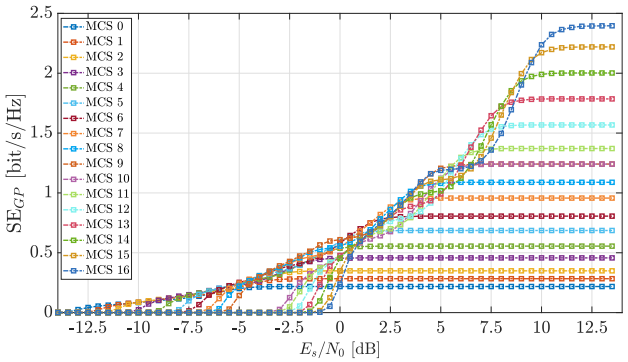

FIGURE 17. SE of HARQ with $N_{ReTx}^{Max} = 3$, for MCS from 0 to 16, in LMS channel with $K = 15$ dB and $s = 50$ km/h. Target BLER 10^{-3}.

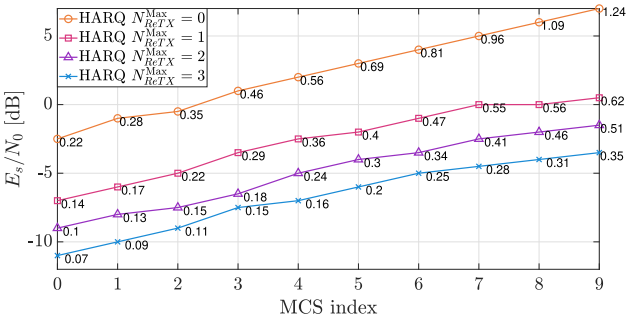

FIGURE 19. E_s/N_0 curves with SE values for each point, in LMS channel with $K = 15$ dB and $s = 50$ km/h. Target BLER 10^{-3}.

be explained by looking at Fig. 17, where the tails of the SE for higher MCSs are higher than the SE of lower MCSs. Even if this SE boost is a positive effect of HARQ, it is worth noting that it requires more retransmissions in order to be reached, and hence a longer latency. To better understand the impact of retransmissions on the LMS channel, we report in Fig. 18 the same curves for AWGN channel. This is an extreme case but could be considered for scenarios where the amount of scattering is extremely low, as for rural areas or aircraft vehicles. In this case, no significant differences can be seen between HARQ and RLC ARQ.

It should be noted that this analysis does not consider the potential challenges of communication at extremely low E_s/N_0, given that 5G NR initial access requires an E_s/N_0 larger than -10 dB [35], [36].

Finally, in Fig. 19 we report both the E_s/N_0 values and the SE for a target BLER of 10^{-3}, for all the different MCSs in Tab. 9, and for every number of transmissions allowed by the HARQ protocol. For a certain range of E_s/N_0 values, the higher MCSs have a higher SE, if more transmissions are used. As an example, MCS 2 with one transmission achieves the target BLER at $E_s/N_0 = -0.5$ dB, and so does MCS 6 with two transmissions. However, MCS 2 has an SE of 0.35 bit/s/Hz, while MCS 6 has an SE of 0.47 bit/s/Hz.

C. IMPERFECT SYNCHRONIZATION

The performance of 5G NTN can be severely weakened by the errors caused by the carrier frequency offset and the Doppler frequency shift, which can be particularly harsh in high frequency bands and with non geostationary orbit satellites, since their speed can be very large (about 7.6 km/s for LEO at 600 km). However, in 5G, most of the frequency offset compensation and, in general, time and frequency synchronization are performed during the initial access. A significant difference between NTN and terrestrial networks is the magnitude of the Doppler rate, i.e., the variation of the Doppler shift in time, which requires additional effort to be mitigated. Various approaches exist and may also exploit the user position provided by the Global Navigation Satellite System (GNSS). 3GPP suggests in [30] to adopt a frequency error of 0.1 ppm to emulate the Residual Frequency Offset (RFO) for the data link simulations, i.e., after initial synchronization. This frequency error translates into an OFDM symbol-based phase variation and ICI. The effect of RFO on PDSCH SE is shown in Fig. 20, reporting results for 16QAM MCSs, since higher modulations are more affected by frequency errors. The curves show how a practical receiver can expect a loss of around 1 dB due to frequency errors. The simulations are obtained by implementing a phase offset compensation via Phase Tracking Reference Signals (PTRS), which are additional 5G pilot symbols designed to

have lower periodicity in time than DMRS. In more detail, firstly we compute the average phase offset in an OFDM symbol via maximum likelihood estimation over the PTRS as

$$\hat{\theta}_i = \text{Arg}\left(\frac{1}{M_i}\sum_{m=0}^{M_i-1} P_m^{(i)} R_m^{(i)*}\right) \tag{5}$$

where $\hat{\theta}_i$ is the estimated phase offset in OFDM symbol i, M_i is the number of PTRS symbols in the i-th OFDM symbol, $P_m^{(i)}$ and $R_m^{(i)}$ are the m-th PTRS symbol and the the m-th received sample, respectively. Arg() is a function that outputs the argument of a complex value, and .* denotes the conjugate operator. Then, we linearly interpolate the obtained sequence of estimated phase offsets to get phase offset estimates also in the OFDM symbols that do not contain PTRS. Finally, we compensate the data symbols with the estimated phase offsets for each OFDM symbol.

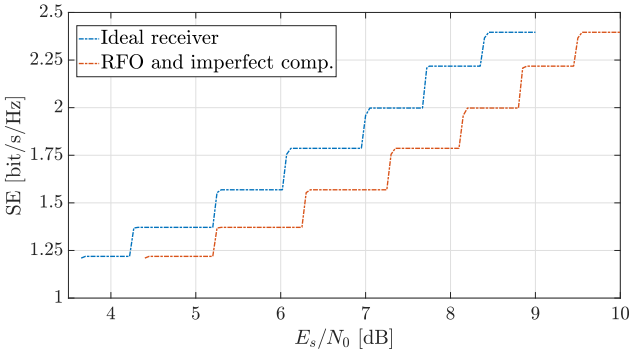

FIGURE 20. SE envelope comparison over AWGN channel for MCS from 10 to 16 (16QAM) and with RFO of 0.1 ppm. Target BLER 10^{-3}. No retransmissions.

D. DISCUSSION

The results presented show that, even for the LMS satellite channel, the advantage provided by HARQ over RLC ARQ is significant in terms of BLER, allowing the system to operate at a much lower E_s/N_0. Also, the latency increase with HARQ (while lowering the E_s/N_0) is lower than the latency increase with RLC ARQ. As a consequence, HARQ is confirmed as the preferred solution also for most NTN applications. Our analysis quantifies the gain, and our open-source simulator can be used to further explore other aspects of interest.

Nonetheless, HARQ is more complex than RLC ARQ because it combines error detection and retransmission with forward error correction, requiring additional processing at the receiver to store and decode partially received data while managing multiple transmissions. This hybrid approach increases computational demands and memory requirements compared to RLC ARQ, which simply retransmits erroneous packets and operates on individual blocks. The support of HARQ is then linked to a cost-performance tradeoff. Considering the main options for NTN equipment, a first feasibility evaluation can be done:

TABLE 11. RLC ARQ latency.

$N_{\text{ReTx}}^{\text{MAX}}$	LEO 1 θ		LEO 2 θ		MEO θ	
	90° [ms]	30° [ms]	90° [ms]	30° [ms]	90° [ms]	30° [ms]
0	2.25	3.75	4.25	6.87	26.87	33.87
1	6.62	11.11	12.62	20.5	80.5	101.5
3	15.37	25.87	29.37	47.75	187.75	236.75
7	32.87	55.37	62.87	102.25	402.25	508.25
31	137.87	232.37	263.87	429.25	1689.25	2130.25

TABLE 12. 5G latency requirements (from [37] and [38]).

Application	Maximum latency
Voice and Videophone	preferred 150 ms, max 400 ms
Interactive games	75 ms
Web-browsing	2-4 sec
Streaming	10 sec
Immersive multi-modal VR	5-10 ms
Remote control robot	1-100 ms
Medical monitoring	100 ms

- Internet of Things (IoT) terminals must be energy efficient, and the complexity is a limiting factor. However, since they do not usually require high throughput, HARQ may still be used allowing stop-and-wait to combine different data retransmissions.
- Handheld terminals can afford a higher complexity, but battery duration is still a design constraint. HARQ may still be helpful in harsh signal propagation conditions, without requiring an excessive increase of the number of processes (reaching very low E_s/N_0 for minimum service, e.g., emergency).
- VSAT terminals for satellite communications typically provide high throughput. These devices may benefit from the adoption of HARQ as they can support features requiring an even higher complexity.

If HARQ complexity is a concern for the on-ground receiver, and if an ACM mechanism is in place, the advantage of HARQ over RLC ARQ in terms of spectral efficiency becomes smaller and limited to the very low E_s/N_0 regime, which may be outside the operational range of interest. RLC ARQ could then become a preferable alternative in NTNs under these conditions:

- LMS channel characterized by a large K-factor;
- Channel state changing slowly w.r.t. ACM loop;
- Receiver with limited complexity or energy consumption constraints.

Clearly, RLC ARQ latency becomes a critical factor, and the number of retransmissions must be carefully managed.

To give a better overview of latency values for RLC ARQ with different orbits and number of retransmissions, we report some representative latency values in Tab. 11. This can be compared to Tab. 12, which contains some typical applications for 5G and the corresponding latencies. To obtain a fairer comparison between the two tables, the values in Tab. 11 should consider at least an additional

propagation delay T_p for the feeder link, and a 5 ms network latency (clause 7.4 in [37]).

VIII. CONCLUSION

In this paper, we analyzed the performance of 5G for Non-Terrestrial Networks by examining the behavior of two New Radio retransmission schemes, HARQ and RLC ARQ, in realistic satellite scenarios. While their performance in terrestrial networks has been well explored, this was not the case for satellite environments.

Firstly, we have investigated the number of HARQ processes required in different scenarios and their relation to the coherence time of the channel. Next, we have developed an open-source simulator that includes all the constituent blocks of the PDSCH physical layer, the retransmission protocols, and the LMS satellite channel. For RLC ARQ we have also presented an analytic approach to estimate the BLER performance over the LMS channel.

Then, we have presented an extensive set of results on the performance of 5G NR HARQ and RLC ARQ over the satellite LMS channel, in terms of BLER, spectral efficiency, and latency. Importantly, both fixed MCS and an ACM mechanism have been considered. Pros and cons of each retransmission protocol have been highlighted and discussed.

The advantages of HARQ over RLC ARQ on the satellite link have been clearly quantified. These insights are valuable as they demonstrate that, even in the complex NTN scenario, characterized by long distances and satellite channels, the HARQ solution can still provide significant gains and enable operation at very low signal-to-noise ratio values, and should be considered the preferred choice for many applications.

From a practical perspective, HARQ increases the complexity of the receiver, requiring extra processing to manage multiple transmissions and to store and decode incomplete received data, which may be problematic for some NTN user equipment. In such cases, if an effective ACM mechanism is available, RLC ARQ could become a viable alternative in NTN. Clearly, signal-to-noise ratio and especially latency become critical factors that must be carefully considered during the design phase of any system.

The presented results and comparisons provide useful guidelines and trade-offs to researchers and space agencies dealing with the use of the 5G NR waveform and protocol stack over Non-Terrestrial Networks. The comprehensive simulator developed in this study enables other researchers to further explore the topic and propose potential improvements. Future research lines include the study of the performance of HARQ and RLC ARQ for very-low Earth orbit satellite constellations (with altitude ranging from 100 km to 450 km), and high-altitude platform systems (with altitudes ranging from 20 km to 50 km), which are recently gaining interest for 5G applications.

ACKNOWLEDGMENT

The authors are grateful to Alberto Ginesi and Stefano Cioni (ESA) for useful discussions. Opinions, interpretations, recommendations, and conclusions presented in this article are those of the authors and are not necessarily endorsed by ESA.

REFERENCES

[1] F. Rinaldi, H.-L. Maattanen, J. Torsner, S. Pizzi, S. Andreev, A. Iera, Y. Koucheryavy, and G. Araniti, "Non-terrestrial networks in 5G & beyond: A survey," *IEEE Access*, vol. 8, pp. 165178–165200, 2020.

[2] *Study on New Radio (NR) to Support Non-Terrestrial Networks (Release 15) V15.4.0*, document TR 38.811, 3GPP, Sophia Antipolis, France, 2020.

[3] M. El Jaafari, N. Chuberre, S. Anjuere, and L. Combelles, "Introduction to the 3GPP-defined NTN standard: A comprehensive view on the 3GPP work on NTN," *Int. J. Satell. Commun. Netw.*, vol. 41, no. 3, pp. 220–238, May 2023. [Online]. Available: https://onlinelibrary.wiley.com/doi/abs/10.1002/sat.1471

[4] A. Guidotti, A. Vanelli-Coralli, M. Conti, S. Andrenacci, S. Chatzinotas, N. Maturo, B. Evans, A. Awoseyila, A. Ugolini, T. Foggi, L. Gaudio, N. Alagha, and S. Cioni, "Architectures and key technical challenges for 5G systems incorporating satellites," *IEEE Trans. Veh. Technol.*, vol. 68, no. 3, pp. 2624–2639, Mar. 2019.

[5] R. Tuninato and R. Garello, "5G NTN primary synchronization signal: An improved detector for handheld devices," *IEEE Open J. Commun. Soc.*, vol. 5, pp. 3792–3803, 2024.

[6] *Physical Layer Procedures for Data; (release 16) V16.2.0*, document TS 38.214-1, 3GPP, Sophia Antipolis, France, 2020.

[7] *Radio Link Control (RLC) Protocol Specification (Release 17) V17.3.0*, document TS 38.322, 3GPP, Sophia Antipolis, France, 2023.

[8] U. Mutlu and Y. Kabalci, "Performance analyses of hybrid-ARQ in fifth generation new radio," in *Proc. 3rd Global Power, Energy Commun. Conf. (GPECOM)*, Oct. 2021, pp. 269–274.

[9] C. Shi, A. Bergstrom, E. Eriksson, P. Frenger, and A. A. Zaidi, "Retransmission schemes for 5G radio interface," in *Proc. IEEE Globecom Workshops (GC Wkshps)*, Dec. 2016, pp. 1–6.

[10] S. R. Khosravirad, K. I. Pedersen, L. Mudolo, and K. Bakowski, "HARQ enriched feedback design for 5G technology," in *Proc. IEEE 84th Veh. Technol. Conf. (VTC-Fall)*, Sep. 2016, pp. 1–5.

[11] G. Berardinelli, S. R. Khosravirad, K. I. Pedersen, F. Frederiksen, and P. Mogensen, "Enabling early HARQ feedback in 5G networks," in *Proc. IEEE 83rd Veh. Technol. Conf. (VTC Spring)*, May 2016, pp. 1–5.

[12] E. Cabrera, G. Fang, and R. Vesilo, "Adaptive hybrid ARQ (A-HARQ) for ultra-reliable communication in 5G," in *Proc. IEEE 85th Veh. Technol. Conf. (VTC Spring)*, Jun. 2017, pp. 1–6.

[13] C.-Y. Liang, M.-R. Li, H.-C. Lee, H.-Y. Lee, and Y.-L. Ueng, "Hardware-friendly LDPC decoding scheduling for 5G HARQ applications," in *Proc. IEEE Int. Conf. Acoust., Speech Signal Process. (ICASSP)*, May 2019, pp. 1418–1422.

[14] J. Sedin, L. Feltrin, and X. Lin, "Throughput and capacity evaluation of 5G new radio non-terrestrial networks with LEO satellites," in *Proc. IEEE Global Commun. Conf. (GLOBECOM)*, Dec. 2020, pp. 1–6.

[15] N. Pachler, I. del Portillo, E. F. Crawley, and B. G. Cameron, "An updated comparison of four low Earth orbit satellite constellation systems to provide global broadband," in *Proc. IEEE Int. Conf. Commun. Workshops (ICC Workshops)*, Jun. 2021, pp. 1–7.

[16] F. Völk, T. Schlichter, S. Kumar, R. T. Schwarz, A. Knopp, M. Hammouda, T. Heyn, J. Querol, S. Chatzinotas, and A. Kapovits, "5G non-terrestrial networks with OpenAirInterface: An experimental study over GEO satellites," *IEEE Access*, vol. 12, pp. 155098–155109, 2024.

[17] S. Kumar, C. K. Sheemar, J. Querol, A. Nik, and S. Chatzinotas, "Experimental study of the effects of RLC modes for 5G-NTN applications using OpenAirInterface5G," in *Proc. IEEE Globecom Workshops (GC Wkshps)*, Dec. 2023, pp. 233–238.

[18] *Discussion on the HARQ Procedure for NTN*, document r1-1906873, ZTE, Reno, NV, USA, 2019.

[19] *Delay-tolerant Re-Transmission Mechanisms in NR-NTN*, document r1-2006327, MediaTek Inc., 2020.

[20] S. Cioni, X. Lin, B. Chamaillard, M. El Jaafari, G. Charbit, and L. Raschkowski, "Physical layer enhancements in 5G-NR for direct access via satellite systems," *Int. J. Satell. Commun. Netw.*, vol. 41, no. 3, pp. 262–275, May 2023.

[21] S. Scalise, H. Ernst, and G. Harles, "Measurement and modeling of the land mobile satellite channel at Ku-band," *IEEE Trans. Veh. Technol.*, vol. 57, no. 2, pp. 693–703, Mar. 2008.

[22] *Recommendation ITU-R P.681-11: Propagation Data Required for the Design Systems in the Land Mobile-Satellite Service*, document 681-11, ITU-R, 2019.
[23] A. Goldsmith, *Wireless Communications*. Cambridge, U.K.: Cambridge Univ. Press, 2005.
[24] *Physical Channels and Modulation (Release 15) V15.2.0*, document TS 38.211, 3GPP, Sophia Antipolis, France, 2018.
[25] *Multiplexing and Channel Coding, ETSI TS 138 212 V15.2.0 (Release 15)*, document TS 38.212, 3GPP, Sophia Antipolis, France, 2018.
[26] *Physical Layer Procedures for Control (Release 17) V17.1.0*, document TS 38.213, 3GPP, Sophia Antipolis, France, 2022.
[27] R. Tuninato, G. Maiolini Caoez, N. Mazzali, and R. Garello. *5G NR NTN Simulator for HARQ and ARQ Performance Evaluation.* Accessed: Mar. 11, 2025. [Online]. Available: https://github.com/RiccardoTuninato/5G-NR-NTN-PDSCH-simulator
[28] E. Dahlman, S. Parkvall, and J. Skold, *5G/5G-Advanced: The New Generation Wireless Access Technology*. Amsterdam, The Netherlands: Elsevier, 2023.
[29] *Medium Access Control (MAC) Protocol Specification (Release 18) V18.1.0*, document TS 38.321, 3GPP, Sophia Antipolis, France, 2024.
[30] *Solutions for NR to Support Non-Terrestrial Networks (NTN) (Release 16) V16.2.0*, document TR 38.821, 3GPP, Sophia Antipolis, France, 2023.
[31] *HARQ Enhancement for NTN*, document r1-1912125, Panasonic, Reno, NV, USA, 2019.
[32] R. H. Clarke, "A statistical theory of mobile-radio reception," *Bell Syst. Tech. J.*, vol. 47, no. 6, pp. 957–1000, Jul. 1968.
[33] Mathworks. *MATLAB 5G Toolbox*. Accessed: Mar. 11, 2025. [Online]. Available: https://www.mathworks.com/products/5g.html
[34] J. G. Proakis and M. Salehi, *Digital Communications*. New York, NY, USA: McGraw-Hill, 2006.
[35] A. Omri, M. Shaqfeh, A. Ali, and H. Alnuweiri, "Synchronization procedure in 5G NR systems," *IEEE Access*, vol. 7, pp. 41286–41295, 2019.
[36] R. Tuninato, D. G. Riviello, R. Garello, B. Melis, and R. Fantini, "A comprehensive study on the synchronization procedure in 5G NR with 3GPP-compliant link-level simulator," *EURASIP J. Wireless Commun. Netw.*, vol. 2023, no. 1, pp. 1–29, Oct. 2023.
[37] *Service Requirements for the 5G System; Stage 1 (Release 20) V20.1.0*, document TS 22.261, 3GPP, Sophia Antipolis, France, 2024.
[38] *Services and Service Capabilities (Release 18) V18.0.01*, document TS 22.105, 3GPP, Sophia Antipolis, France, 2024.

RICCARDO TUNINATO (Graduate Student Member, IEEE) received the Ph.D. degree in electrical, electronic and communications engineering from the Politecnico di Torino in 2024. During the Ph.D. degree, he spent time as a Visiting Student with Cal State LA, Los Angeles. He started his current position at European Space Agency, as a Communication Systems and Technologies Engineer, in 2024. His research interests include the study and analysis of the physical layer of communication systems, mainly related to the 5G standard and satellite communications. In particular, he investigated the techniques for synchronization and initial access, and the beamforming techniques for massive MIMO systems.

GABRIEL MAIOLINI CAPEZ (Graduate Student Member, IEEE) received the master's degree in communications and computer networks engineering from the Politecnico di Torino, where he is currently pursuing the Ph.D. degree in electronics and telecommunications engineering. He has wide domain experience in satellite communication systems, space networks, and digital signal processing algorithms. His research interests include innovative communication and ranging systems for space-to-space and space-to-ground applications, including constellation design.

NICOLÒ MAZZALI (Member, IEEE) received the master's degree (cum laude) in telecommunications engineering and the Ph.D. degree in information technologies from the University of Parma, Italy, in 2009 and 2013, respectively. He was a Visiting Postdoctoral Researcher with the Department of Signals and Systems, Chalmers University of Technology, Gothenburg, Sweden, and a Research Associate with the Interdisciplinary Centre for Security, Reliability and Trust, University of Luxembourg, Luxembourg. Since 2018, he has been a Communication Systems and Technologies Engineer with the Directorate of Technology, Engineering, and Quality, European Space Agency. His research interests include signal processing for wireless, satellite, and free-space optical communications, synchronization, and estimation theory.

ROBERTO GARELLO (Senior Member, IEEE) received the Ph.D. degree in electronic engineering from the Politecnico di Torino, in 1994, with a thesis on error correction coding. During the Ph.D. degree, he was a Visiting Student with MIT, Cambridge, and ETH, Zürich. From 1994 to 1997, he was with Marconi Communications, Genoa. From 1998 to 2001, he was an Associate Professor with the University of Ancona. Since November 2001, he has been an Associate Professor with the Department of Electronics and Telecommunications, Politecnico di Torino. In 2017, he was an Adjunct Professor with California State University, Los Angeles. His research interests include space communication systems, 5G and beyond mobile networks, and channel coding. On these topics, he has co-authored more than 150 articles. He has been the Project Manager of more than 40 research projects and the advisor of 12 Ph.D. students.